Transition Met Chem (2014) 39:917–924
DOI 10.1007/s11243-014-9876-z

Manganese(II) complexes of quinoline derivatives: characterization, catalase activity, interaction with mitochondria and anticancer activity

Zhi-Wei Wang · Qiu-Yun Chen · Qing-Shan Liu

Received: 17 June 2014 / Accepted: 21 August 2014 / Published online: 4 September 2014

Abstract In order to find mitochondria-targeted mimics of catalase that can attenuate the metabolism of oxygen for cancer chemotherapy, two complexes $[Mn(QA)Cl_2]$ and $[Mn(QA)(OAc)(H_2O)_2](OAc)$ (QA = 2-di(picolyl)amine-*N*-(quinoline-8-yl)acetamide) were synthesized and characterized by spectroscopic methods. In addition, the crystal structure of $[Mn(QA)Cl_2]$ shows that the Mn(II) atom is coordinated by three N atoms (N1, N2,and N3), and one oxygen atom (O1) of the ligand QA, plus two chloride atoms (Cl1 and Cl2), forming a distorted octahedral geometry. The complex $[Mn(QA)(OAc)(H_2O)_2](OAc)$ could disproportionate H_2O_2 in Tris–HCl solution at 37 °C, with $K_{cat}/K_M = 9{,}226$. Furthermore, both Mn(II) complexes were found to be active against the proliferation of HepG-2 cells and could attenuate the swelling of calcium-overloaded mitochondria. These results demonstrate that Mn(II) complexes of quinoline derivatives have potential as attenuators of the absorption of Ca^{2+} in mitochondria and can interfere with the metabolism of O_2 for cancer chemotherapy.

Electronic supplementary material The online version of this article (doi:10.1007/s11243-014-9876-z) contains supplementary material, which is available to authorized users.

Z.-W. Wang · Q.-Y. Chen (✉) · Q.-S. Liu
School of Chemistry and Chemical Engineering, Jiangsu University, Zhenjiang 212013, P.R.China
e-mail: chenqy@ujs.edu.cn

Q.-Y. Chen
State Key Laboratory of Coordination Chemistry, Nanjing University, Nanjing 210093, P.R.China

Introduction

The quinoline nucleus is a common substructure of many biologically active compounds and occupies an important position in medicinally relevant heterocyclic systems [1–3]. Tasquinimod, an oral quinolone-3-carboxamide with antitumor activity that is currently under investigation in preclinical models of prostate cancer, has been tested in patients with minimally symptomatic castration-resistant prostate cancer, showing promising inhibitory effects on the occurrence of metastasis. Although cisplatin and its analogs have several major drawbacks, such as cumulative nephrotoxicity and ototoxicity as well as inherent or treatment-induced resistance, these drugs have provided the motivation for developing novel metal complexes as anticancer agents [4, 5]. Di(picolyl)amine (dpa) has been used as a neutral, nondeprotonated chelating ligand capable of complexing Zn(II), Cu(II), Fe(II, III), and Mn(II) atoms to recognize proteins [6]. Previously, we found that a Mn(II) complex, $[Mn(Adpa)(Cl)(H_2O)]$ (Adpa = bis(pyridylmethyl)amino-2-propionic acid), could both target mitochondria and inhibit the proliferation of human glioma cells (U251) with IC_{50} value of 9.5 μM in vitro [7]. Hence, there is the possibility that special Mn(II) complexes could target cancer cells through an ATP-related Ca transporter. Mitochondrial Ca^{2+} loading has profound consequences for mitochondrial function, such as regulating cellular respiration and mediating cell death by apoptosis or necrosis [8, 9]. The ability of the Ca^{2+} ion to regulate both cell death and proliferation offers the possibility of new drug targets in cancer. In addition to attenuation of the absorption of calcium in mitochondria, Mn(II) complexes of di(picolyl)amine derivatives have been reported as models for nonheme dioxygenase [10]. For example, Mn(II) complexes of bis(2-pyridylmethyl)benzylamine can

react with H_2O_2, resulting in intramolecular aromatic hydroxylation (pro-oxidant) [11]. The manganese(II) complex $[Mn_2(\mu\text{-}OAc)_3L_2]^+$ (L = bis(pyridyl methyl)amine) and aminopyridine manganese(II) complexes were found to disproportionate H_2O_2 and produce highly valued intermediates [12, 13]. Hence, manganese(II) complexes of bis(2-pyridylmethyl)amine derivatives may disproportionate H_2O_2 or react with H_2O_2 to produce an oxidant. Cellular levels of H_2O_2 directly or indirectly play a key role in malignant transformation and in sensitizing cancer cells to death. During the overexpression of H_2O_2-detoxifying enzymes or catalase in vivo, H_2O_2 concentration was observed to decrease, and the cancer cells reverted to normal appearance [14]. Cancer cells are more susceptible to H_2O_2-induced cell death than are normal cells. Therefore, manganese(II) complexes of N-substituted di(picolyl)amines could act as multifunctional complexes that inhibit the proliferation of cancer cells by attenuating the absorption of Ca^{2+} in mitochondria as well as disproportionation of H_2O_2. The combination of the quinoline group, Mn(II) ligand and di(picolyl)amine, could give multifunctional mimics of catalase against cancer cells. Here, we report the syntheses, characterization, interaction with ct-DNA and mitochondria, catalase activities, and antitumor activities of $[Mn(QA)Cl_2]$ (**1**) and $[Mn(QA)(OAc)(H_2O)_2](OAc)$ (**2**) (QA = 2-di(picolyl)amine- *N*-(quinoline-8-yl)acetamide).

Experimental

Materials and measurements

All chemicals and solvents used for syntheses were of reagent grade and used without further purification. Tris(hydroxymethyl) aminomethane (tris) was obtained from Sigma. Water was purified with a Millipore Milli-Q system. The C, H, and N microanalyses were performed on a Vario EL elemental analyzer. Electronic absorption spectra were recorded in the 900–190-nm region using a Varian cary 50-BIO UV–VIS spectrophotometer. Infrared spectra were recorded on a Nicolet-470 spectrophotometer in the wavenumber range of 4,000–400 cm^{-1} using KBr pellets.

Synthesis of 2-chloro-*N*-(quinol-8-yl)-acetamide

A solution of 2-chloroacetyl chloride (0.54 g, 4.8 mmol) was dissolved in CH_2Cl_2 (10 ml) and then added dropwise to a cooled stirred solution of 8-aminoquinoline (0.58 g, 4 mmol) and Et_3N (0.4 g, 4 mmol) in CH_2Cl_2 (20 ml) within 1 h. After being stirred for 2 h at room temperature, the mixture was removed under reduced pressure to obtain a white solid, which was purified by silica gel column chromatography using ethyl acetate and petroleum ether (3:1, v/v) as the eluent to afford the product. Yield 0.75 g (85 %). Anal. Calc. for $C_{11}H_9N_2OCl$: C 59.9 %, H 4.1 %, N 12.7 %. Found: C 59.8 %, H 3.9 %, N 12.6 %.

Synthesis of 2-di(picolyl)amine-*N*-(quinoline-8-yl)acetamide

2-Chloro-*N*-(quinol-8-yl)-acetamide (0.75 g, 3.5 mmol), di(picolyl)amine (0.56 g, 3 mmol), Et_3N (0.3 g, 3 mmol), and potassium iodide (20 mg) were dissolved in acetonitrile (30 ml), and the mixture was stirred under reflux for 10 h under a nitrogen atmosphere. The mixture was cooled to room temperature, and the solvent was removed to obtain a yellow oil, which was purified by silica gel column chromatography using ethyl acetate as eluent to afford the product. Yield 0.8 g (70 %). ^{1}HNMR (400 MHz, $CDCl_3$): δ 3.56 (*s*, 2H), 4.04 (*s*, 4H), 7.15–7.19 (*m*, 2H), 7.51–7.55 (*m*, 3H), 7.66 (*d*, $J = 7.7$ Hz, 2H), 8.00 (*d*, $J = 7.9$ Hz, 2H), 8.21 (*d*, $J = 5.9$ Hz, 1H), 8.54 (*d*, $J = 4.9$ Hz, 2H), 8.77–8.80 (*m*, 1H), 8.96 (*d*, $J = 5.9$ Hz, 1H), 11.62(*s*, 1H). ESI–MS (in CH_3OH): *m/z* 384.31 $[QA + H]^+$. IR (KBr, cm^{-1}): 3,310 (*m*), 3,069 (*m*), 2,926 (*m*), 2,858 (*m*), 1,670 (*s*), 1,591 (*s*), 1,541 (*m*), 1,474 (*m*), 1,432 (*m*), 760 (*s*). UV–vis (EtOH/nm) ($\varepsilon \times 10^4$/dm^3 mol^{-1} cm^{-1}): 208 (5.6), 240 (6.6), 260 (2.3), 316 (1.2).

Synthesis of complex **1**

To a stirred solution of QA (380 mg, 1 mmol) in ethanol (5 ml), a solution of $MnCl_2{\cdot}4H_2O$ (198 mg, 1 mmol) in ethanol (5 ml) was added dropwise. The mixture was stirred at 80 °C for 2 h and then cooled to room temperature. After the solution was diffused with ethyl ether, a yellow solid was obtained. Yield 0.40 g (80 %). Anal. Calc. for $C_{23}H_{21}Cl_2MnN_5O$: C 54.2 %. H 4.1 %, N 13.7 %. Found: C 54.3 %, H 4.0 %, N 14.0 %. IR (KBr, cm^{-1}): 3,298 (*m*), 3,069 (*m*), 2,908 (*m*), 1,660 (*s*), 1,591 (*s*), 1,542 (*m*), 1,474 (*m*), 1,430 (*m*), 764 (*s*). UV–vis (EtOH/nm) ($\varepsilon \times 10^4$/dm^3 mol^{-1} cm^{-1}): 209 (4.2), 240 (3.5), 258 (2.7), 316 (0.8).

Synthesis of complex **2**

To a stirred solution of QA (380 mg, 1 mmol) in ethanol (5 ml), a solution of $MnOAc_2{\cdot}4H_2O$ (250 mg, 1 mmol) in ethanol (5 ml) was added dropwise. The mixture was stirred at 80 °C for 2 h and then cooled to room temperature. After the solution was diffused with ethyl ether, a brown solid was obtained and dried. Yield 0.44 g (75 %). Anal. Calc. for $C_{27}H_{31}MnN_5O_7$: C 54.7 %. H 5.2 %, N 11.8 %. Found: C 53.2 %, H 5.1 %, N 12.3 %. IR (KBr,

cm^{-1}): 3,424 (*m*), 3,060 (*m*), 2,908 (*m*), 1,558 (*s*), 1,423 (*s*), 768 (s). ESI–MS (in CH_3OH): *m/z* 437.18 $[Mn(QA-H)]^+$ (38 %), 468.22 $[Mn(QA-H)(CH_3OH)]^+$ (100 %). UV–vis (EtOH/nm) ($\varepsilon \times 10^4/dm^3\ mol^{-1}\ cm^{-1}$): 210 (2.3), 257 (2.0), 358 (0.4).

X-ray crystallography

Crystallographic data for $[(QA)MnCl_2]$ (1) are listed in Table 1. A colorless prism crystal of the complex was selected for lattice parameter determination and collection of intensity at 298 K on a Rigaku Mercury2 CCD Area Detector with monochromatized Mo Kα radiation ($\lambda = 0.0710747$ nm). A total of 6,893 reflections were collected, of which 4,449 reflections were observed with $I > 2\sigma(I)$. The structure was solved using direct methods with the SHELXS-97 program [15], and the nonhydrogen atoms were located from the trial structure and then refined anisotropically with SHELXTL using full-matrix least-squares procedures based on F^2 values. The hydrogen atom positions were fixed geometrically at calculated distances and allowed to ride on the parent atoms. All calculations were performed using the SHELX-97 programs.

Table 1 Crystal data and structural refinements of complex **1**

Empirical formula	$C_{23}H_{21}Cl_2MnN_5O$
Color/shape	Colorless/prism
Formula weight	509.29
Temperature/K	293(2)
Wavelength/nm	0.71073
Crystal system/space group	Orthorhombic/P 21 21 21
a/nm	7.5725(15)
b/nm	9.0909(18)
c/nm	32.768(7)
α(°)	90.00
β(°)	90.00
γ(°)	90.00
Final *R* indices $[I > 2\sigma(I)]$	$R_1 = 0.0426$; $wR_2 = 0.0812$
Volume/nm^3	2,255.8(8)
Z	4
Density (calculated)/$(g \cdot cm^{-3})$	1.500
Absorption coefficient/mm^{-1}	0.848
F(000)	1,044
Crystal size/mm	0.32 × 0.3 × 0.28
θ range for data collection/(°)	3.27 to 26.02
Index ranges	$-6 \le h \le 9, -9 \le k \le 11, -26 \le l \le 40$
Reflections collected	6,893
Observed reflections $[I > 2\sigma(I)]$	4,449
Goodness of fit on F^2	1.051
R indices (all data)	$R_1 = 0.0498$; $wR_2 = 0.0886$

Catalase-like activity

All of the reactions between the complexes and dihydrogen peroxide were performed in buffered (Tris/Tris–HCl, 0.1 M, NaCl, 0.1 M, and pH = 7.4) or water solutions at 0 or 37 °C. The reactivity of the complexes with H_2O_2 was first investigated in water via UV–vis spectroscopy titration at 37 °C. After a solution (10 ml) of the complex (0.1 M) was stirred at 0 and 37 °C for 30 min, 0.5 ml of H_2O_2 aqueous solution (30 %) was added, and the spectra were recorded at 2 min intervals at 37 °C. Volumetric measurements of the evolved dioxygen produced during the reaction of the complexes with H_2O_2 were taken in triplicate as follows: a 10-ml round-bottom flask containing the required complex (1.0×10^{-3} M, 3.0 ml) in MeCN solvent (or a buffered system) was placed in an ice (273.0 ± 0.1 K) bath. The flask was closed with a rubber septum, and a cannula was used to connect it to an inverted graduated buret, filled with water. While the solution containing the complex was being stirred, an aliquot of 0.5 ml of H_2O_2 aqueous solution was added through the septum using a microsyringe. The volume of oxygen produced was measured in the buret. The kinetics measurements for both complexes were taken in MeCN solution at 37 °C. Different concentrations of H_2O_2 were prepared by diluting a 30 % H_2O_2 aqueous solution with acetonitrile or Tris–HCl buffer solution. The optimum reaction order of the substrate with respect to the complexes was determined by reacting different concentrations of each complex with a constant concentration of substrate. Similarly, the optimum reaction order of the complexes with respect to the substrate was determined by reacting different concentrations of substrate with a constant concentration of the complex.

Cytotoxicity assays

The cytotoxicity assays were carried using HepG-2 cell lines. HepG-2 cells were cultured in DMEM medium (dulbecco's minimum essential medium) containing 10 % (v/v) heat-inactivated fetal bovine serum, antibiotics (100 U ml^{-1} penicillin and 100 U ml^{-1} streptomycin). All cells were grown at 37 °C in a humidified atmosphere in the presence of 5 % CO_2. Cells were seeded at a density of 4×10^4 cells/ml into 96-sterile-well plates and grown in 5 % CO_2 at 37 °C. The test complexes were dissolved in DMSO and diluted with culture media. After 24 h, the required complex was added, and the samples were kept for 48 h. Cell viability was determined by the 3-[4,5-dimethylthiazol-2-yl]-2,5- diphenpyltetrazolium bromide (MTT) assay by measuring the absorbance at 570 nm with an ELISA reader. IC_{50} was calculated using software provided by Nanjing University. Each test was performed in triplicate. Comparisons were made by one-way analysis of

variance. Differences were considered to be significant when $p<0.05$. All experiments were repeated at least three times.

Mitochondrial swelling

Liver mitochondria were isolated by conventional differential centrifugation from adult rats [16]. The livers were homogenized in 250-mM sucrose, 1-mM EGTA (ethylenebis(oxyethylenenitrilo)tetraacetic acid), and 10-mM HEPES (4-(2-hydroxyethyl)piperazine-1-ethanesulfonic acid) buffer (pH 7.4). The mitochondrial suspension was washed twice with the same medium containing 0.1-mM EGTA, and the pellet was resuspended in 250-mM sucrose to a final protein concentration of 80–100 mg/ml. Mitochondria (0.4 mg of protein) were incubated in 1.5 ml of a medium containing 125-mM sucrose, 65-mM KCl, 10-mM HEPES–KOH, pH 7.4, and 5-mM potassium succinate (+2.5 μM rotenone) at 25 °C. Each test complex was dissolved in H_2O and diluted with culture media. Various concentrations of the tested complexes (1–100 μM) were added to the assay mixture. Swelling was initiated by the addition of 50-μM $CaCl_2$ to the sample cuvette at 25 °C. Ciclosporin A (5 μM) was used as a positive reference. Mitochondrial swelling was estimated from the decrease in absorbance at 540 nm measured with a Hitachi U-2000 spectrophotometer. The extent of mitochondrial swelling was assayed by measuring the decrease in absorbance (A) at 540 nm, and the inhibitory rate of mitochondrial swelling was calculated as follows: $(\Delta A_{control}-\Delta A_{drug})/\Delta A_{control} \times 100\ \%$, $\Delta A = \Delta A_{0min}-A$.

Results and discussion

Synthesis and characterization of the complexes

2-Di(picolyl)amine-*N*-(quinoline-8-yl)acetamide (QA) was synthesized by conjugating dpa (di(picolyl)amine) and 2-chloro-*N*-(quinol-8-yl)acetamide, which was prepared from 8-aminoquinoline and 2-chloroacetyl chloride. Complexes **1** and **2** were synthesized by treating QA with $MnCl_2{\cdot}4H_2O$ and $MnOAc_2{\cdot}4H_2O$, respectively, in 1:1 molar ratio in ethanol solution. Both complexes show a typical absorption band at 260 nm due to a $\pi \rightarrow \pi^*$ transition involving the pyridine groups of the ligand. Two obvious strong bands at 240 nm and 316 nm are attributed to the $\pi \rightarrow \pi^*$ and $n \rightarrow \pi^*$ transitions, respectively, of the ligands. The typical absorption of the quinoline ring in complex **2** is shifted to 358 nm compared to the free ligand and complex **1** with a absorption at 316 nm. This suggests that the quinoline nitrogen may be coordinated with manganese in complex **2** (Fig. S1). The FTIR spectrum of the free QA shows two pyridyl ring bands at approximately 1,591 and 1,541 cm^{-1}; strong peaks at 3,310 and 1,670 cm^{-1} were assigned to the ν(N–H) and ν(C=O) stretching vibration frequencies, respectively. The out-of-plane deformation vibration of the pyridyl ring in the free ligand occurred at 760 cm^{-1} and is shifted to 764 and 768 cm^{-1} in complexes **1** and **2**, respectively (Fig. S2). These shifts indicate that the pyridyl nitrogen atoms are coordinated to the metal in both complexes [17, 18]. The shift toward lower frequencies for the ν(C=O) vibration from 1,670 cm^{-1} in the free ligand to 1,660 cm^{-1} in complex **1** indicates that the oxygen atom also coordinates to the metal, which is consistent with the crystal structure. A strong peak at 3,400 cm^{-1} for complex **2** is assigned to ν(O–H) asymmetric stretching frequencies, showing the presence of water molecules. Complex **2** shows $\nu_{as}(OAc^-)$ at 1,558 cm^{-1} and $\nu_{as}(OAc^-)$ at 1,423 cm^{-1}, indicating the presence of carboxylate. Thermal analysis (TG) curves of complex **2** in the range 0–1,000 °C are shown in Fig. S3. The thermal decomposition of the $[Mn(QA)(OAc)(H_2O)_2](OAc)$ (**2**) proceeds in two distinguishable steps. The first falls in the range of 25–210 °C, which is assigned to the loss of two H_2O ligands with a weight loss 6.20 % (calcd. 6.08 %). A further 52.62 % weight loss in the range of 210–440 °C corresponds to two CH_3COO^- and di(pyridylmethyl)amine groups from the ligand (calcd 53.37 %). The thermal decomposition data are consistent with the proposed structure of complex **2**. In the mass spectrum of $[Mn(QA)(OAc)(H_2O)_2](OAc)$ (**2**), the main peak at $m/z = 468.22$ (100 %) corresponds to species $[Mn(QA\text{-}H)(CH_3OH)]^+$, while a peak at $m/z = 437.18$ (38 %) is assigned to species $[Mn(QA\text{-}H)]^+$ (Fig. S4). ES-MS data indicate that complex **2** is a mononuclear manganese(II) species.

Crystal structure of complex **1**

The crystal structure of complex **1** with the atomic labeling scheme is shown in Fig. 1, and selected bond lengths and angles are listed in Table 2. QA acts as a tetradentate ligand toward the Mn(II) atom, which is coordinated by three N atoms (N1, N2, and N3), one oxygen atom (O1) of QA and two chloride ligands (Cl1, Cl2), resulting in a six coordinate mononuclear Mn(II) complex. Complex **1** shows a distorted octahedral geometry similar to a previous reported dinuclear manganese(II) complex $[Mn(Aldpa)Cl(\mu\text{-}Cl)]_2$ (Aldpa = *N*-allyl di(picolyl)amine) [19]. Atoms Cl2, N3, N1, and N2 form the equatorial tetragonal plane (mean deviation 0.0327 Å), while Cl1 and O1 occupy the apical positions. The Mn(II) atom is shifted by 0.3993 Å out of the equatorial plane toward Cl1. The Mn(1)–Cl(1) and Mn(1)–O(1) bond distances are 2.4496 (9) Å and 2.294 (2) Å, respectively, and the Cl(1)–Mn(1)–O(1) angle is 166.17 (6)°.

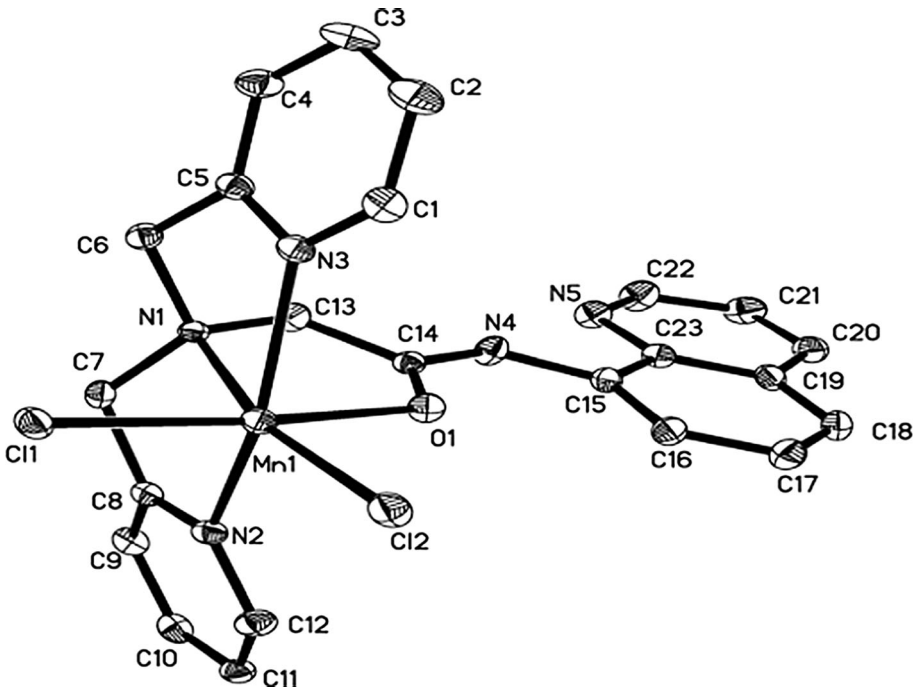

Fig. 1 Crystal structure of complex **1**. Thermal ellipsoids are drawn at 30 % probability; hydrogen atoms are omitted

Table 2 Selected bond lengths (nm) and bond angles (°) for complex **1**

Mn(1)–N(3)	2.278(2)	O(1)–Mn(1)–N(2)	78.58(8)
Mn(1)–O(1)	2.294(2)	N(3)–Mn(1)–Cl(2)	103.25(7)
Mn(1)–N(2)	2.298(2)	O(1)–Mn(1)–Cl(2)	92.34(6)
Mn(1)–Cl(2)	2.3819(9)	N(2)–Mn(1)–Cl(2)	109.29(7)
Mn(1)–N(1)	2.379(2)	N(3)–Mn(1)–N(1)	71.95(8)
Mn(1)–Cl(1)	2.4496(9)	O(1)–Mn(1)–N(1)	73.25(8)
N(3)–Mn(1)–O(1)	84.45(8)	N(2)–Mn(1)–N(1)	72.46(9)
N(3)–Mn(1)–N(2)	143.66(9)	Cl(2)–Mn(1)–N(1)	165.02(6)
N(3)–Mn(1)–Cl(1)	94.84(7)	O(1)–Mn(1)–Cl(1)	166.17(6)
N(2)–Mn(1)–Cl(1)	94.31(7)	Cl(2)–Mn(1)–Cl(1)	101.24(3)
N(1)–Mn(1)–Cl(1)	93.37(6)		

Catalase-like activity

A kinetic study of H_2O_2 disproportionation was carried out by measuring the volume of O_2 evolved in the presence of these complexes. The H_2O_2 disproportionation promoted by complexes **1** and **2** was carried out in MeCN at 37 °C (Fig. 2). Less O_2 evolution was observed when complex **1** was incubated with H_2O_2 compared to complex **2**, due to the presence of a bridging μ-Cl^- ligand in complex **1** [20–22]. Complex **2** in MeCN and buffered solution at 37 °C was a better catalyst for O_2 evolution (Fig. 3). The plot of the initial rate *versus* the concentration of the H_2O_2 was fitted using the Hill Eq. (1) (Fig. S5, Fig. S6).

$$V_0 = V_{max}[s]^n/(K_m + [s]^n) \quad (1)$$

$$K_{cat} = V_{max}/[E_t] \quad (2)$$

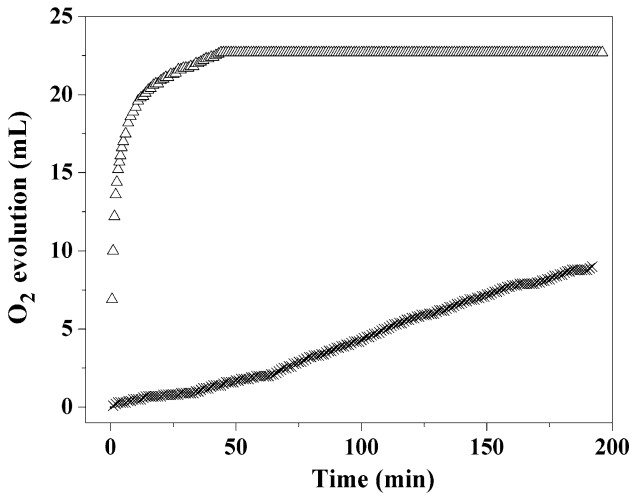

Fig. 2 Rates of the O_2 evolution of the complexes at 37 °C in MeCN, [complex] = 1 mM, 0.5 mL of 30 % H_2O_2 aqueous solution, V_{MeCN} = 5 mL. Complex **2** (*triangle*), complex **1** (*cross*)

The parameter K_{cat} was calculated with the Eq. (2) [17, 18]. The maximum O_2 evolution rates were about 23.4 and 10.3 mM s^{-1} for complex **2** at 37 °C in MeCN and in Tris–HCl solution, respectively, which is larger than the previously reported $[Mn_2(Adpa)_2(OAc)(H_2O)_2](OAc)$ (5.4 mM s^{-1} at 37 °C in Tris–HCl solution) [23]. The Hill constants obtained for complex **2** both in MeCN and in buffered solutions were 3.6 ± 0.58 and 1.8 ± 0.34, respectively, showing that complex **2** can form a high value intermediate when it reacts with H_2O_2 [24]. Complex **2** exhibits high affinity for dihydrogen peroxide with the K_m value of 3.1 mM in Tris–HCl. The

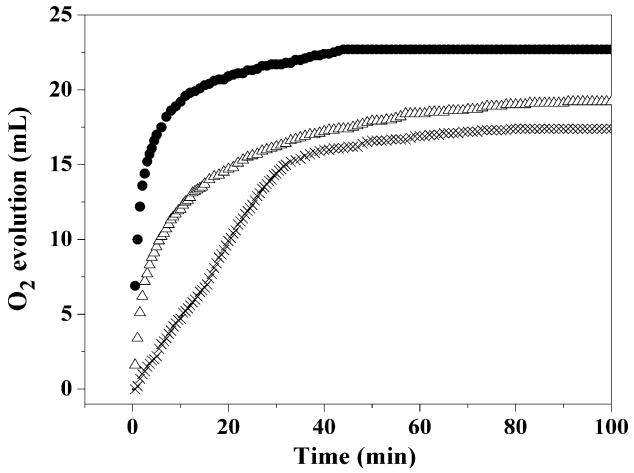

Fig. 3 Rates of the O_2 evolution of complex **2** at different conditions, 0.5 mL of 30 % H_2O_2 aqueous solution, $V_{solvent} = 5$ mL. [complex **2**] = 0.34 mM, 37 °C in MeCN (*filled circle*), [complex **2**] = 1 mM, 37 °C in Tris–HCl (*triangle*), 0 °C in Tris–HCl (*cross*)

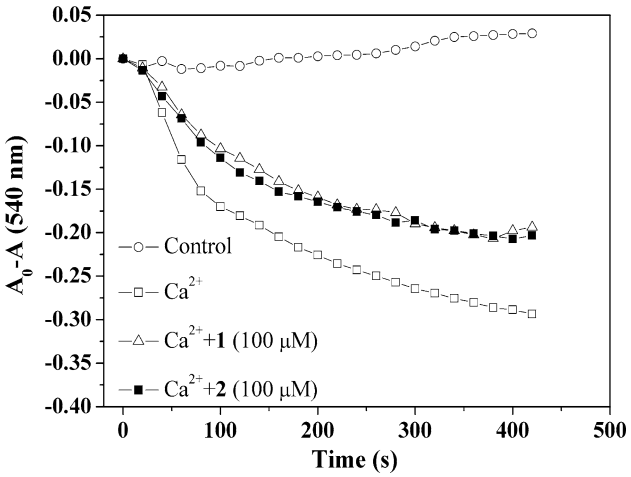

Fig. 4 Inhibition for complexes **1** and **2** on the Ca^{2+}-induced mitochondria swelling

turnover number K_{cat} of complex **2** in MeCN and Tris–HCl solutions is 65 and 28.6 s^{-1}, respectively, indicating that complex **2** is a good catalase mimic. The values of k_{cat}/K_M for complex **2** in MeCN and Tris–HCl are 81,250 and 9,226, respectively, which is higher than most reported Mn(II) complexes [25–28] (Table 3). The conditions of the reaction carried out at 37 °C in Tris–HCl solution are close to those found in cultured cells (37 °C, pH 7.0), suggesting that the complex **2** might also show good catalase activity in vivo.

Interactions with mitochondria

Mitochondrial swelling is an important method to detect mitochondrial functions [29]. The interactions of complexes **1** and **2** with mitochondria were studied by measuring the Ca^{2+}-loaded mitochondrial swelling (Fig. 4). Complexes **1** and **2** (100 μM) can inhibit the swelling of calcium-overloaded mitochondria, indicating that an interaction between the Mn(II) complexes and mitochondria takes place. Mitochondria are involved in the maintenance of intracellular Ca^{2+} homeostasis. One feature of tumor cells is their dependence on glycolysis for ATP generation, which induces the release of Ca^{2+} from the endoplasmic reticulum and leads to enhanced uptake of Ca^{2+} by mitochondria. Both complexes can inhibit the swelling of Ca^{2+}-overloaded mitochondria, indicating that they may interfere with the Ca^{2+} transport system, which is similar to the complex [Mn(Adpa)(Cl)(H_2O)] [7]. Comparing with manganese(II) complexes of N-substituted di(picolyl)amines as previously reported [7, 19, 23], it is found that only mononuclear complexes of dpaMn (dpa = di(picolyl)amine) can inhibit the swelling of calcium-overloaded mitochondria (Scheme 1), while the polynuclear Mn(II) complexes with same ligands show no inhibition on the swelling of calcium-overloaded mitochondria [23]. We deduce that the structures of these Mn(II) complexes may be the key factor for their attenuation of mitochondrial swelling.

Inhibition of cancer cell proliferation

Complexes **1** and **2** were studied for their antitumor activity in vitro by determining their inhibition against growth of cancer cells HepG-2 using the method of MTT reduction. 5-Fluorouracil was used as a positive control for

Table 3 Catalytic activity of manganese catalase and synthetic catalase mimics

Complex	K_M (mM)	k_{cat} (s^{-1})	k_{cat}/K_M (s^{-1} M^{-1})	Hill constant n	Ref
Thermus thermophilus catalase	83	2.6×10^5	3.1×10^6	–	[21]
Thermoleophilum album catalase	15	2.6×10^4	1.7×10^6	–	[22]
$[Mn_2(bpia)_2(\mu\text{-}OAc)_2](ClO_4)_2$	31.5	1,070	34,000	–	[23]
$[Mn^{IV}salpn(\mu\text{-}O)]_2$	250	250	1,000	–	[24]
$[(Adpa)_2Mn_2(\mu\text{-}OAc)](OAc)$ (in MeCN)	1.44 ± 0.27	6.28	4,361.1	3.44 ± 0.58	[19]
$[(Adpa)_2Mn_2(\mu\text{-}OAc)](OAc)$ (in Tris–HCl)	1.76 ± 0.32	9.88	5,615.8	3.24 ± 0.37	[19]
Complex **2** (in MeCN)	0.8	65	81,250	3.6 ± 0.58	This work
Complex **2** (in Tris–HCl)	3.1	28.6	9,226	1.8 ± 0.34	This work

Scheme 1 Mn(II) complexes that can attenuate the swelling of calcium-overloaded mitochondria and signal the apoptosis of cancer cells

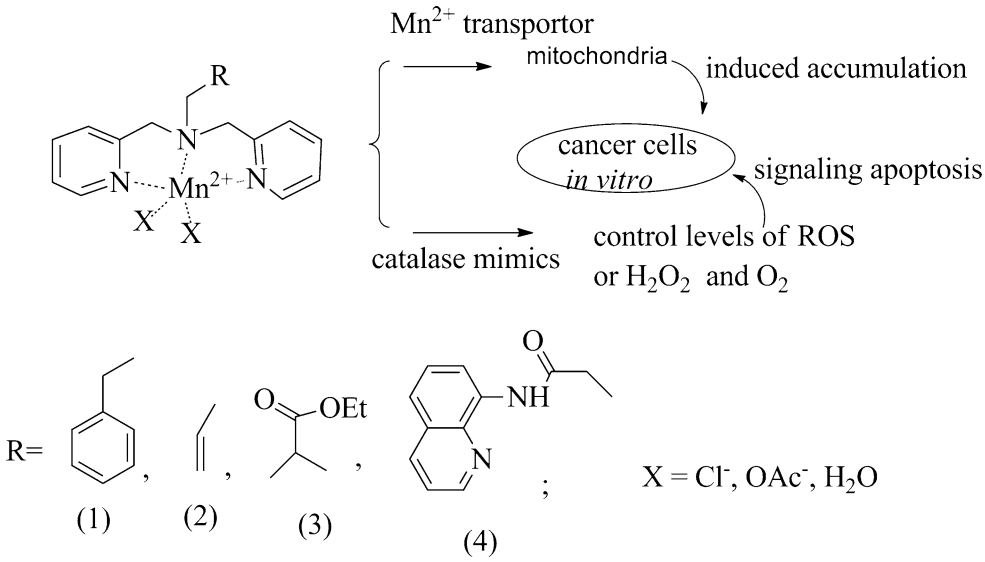

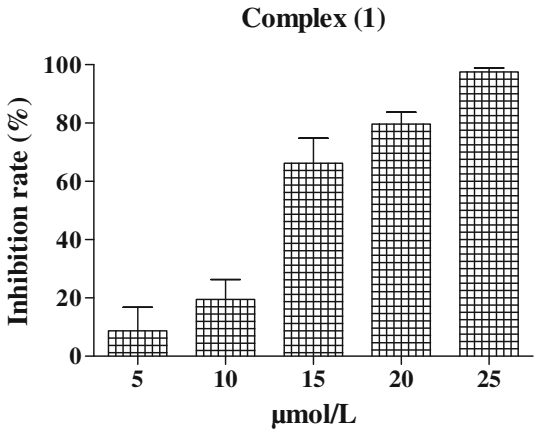

Fig. 5 Concentration-dependent inhibition activities of complex **1** on HepG-2 cell lines. The samples were kept with the complex for 48 h. All experiments were repeated at least three times

cytotoxicity [30]. Both complexes were active against HepG-2 cells, giving IC_{50} values of 11.03 and 52.24 μM, respectively, for complexes **1** and **2** (Fig. 5, Fig. S7 and Table S1). Since H_2O_2 is considered to be a mediator of apoptotic cell death, the elimination of the H_2O_2 is important for protection against oxidative stress. The different IC_{50} values of complexes **1** and **2** are possibly due to their H_2O_2 discriminating ability, which may affect the metabolism of oxygen and the production of ROS signaling apoptosis in cancer cells. Attenuation of the functions of the mitochondria, the antioxidant properties of these manganese(II) complexes, and their catalase activities may all be important factors in their anticancer activities. Considering the IC_{50} values and the effect on mitochondria, we deduce that the complex **2** could be used as a low toxicity complex to attenuate the metabolism of oxygen for cancer recovery chemotherapy in the future.

Conclusion

The Mn(II) complexes $[Mn(QA)Cl_2]$ (**1**) and $[Mn(QA)(OAc)(H_2O)_2](OAc)$ (**2**) are both active against HepG-2 cells, with IC_{50} values of 11.03 μM and 52.24 μM. Both complexes exhibit good inhibition of the swelling of calcium-overloaded mitochondria. In particular, the complex **2** is a good mimic of catalase, so that it can be used as a mitochondria-targeted catalase mimic to attenuate the metabolism of oxygen. Cancer cells use O_2 to generate excessive levels of ROS and H_2O_2. The alteration in the metabolism of O_2 by catalase mimics plays an important role in carcinogenesis. We suggest that the Mn(II) complexes of quinoline derivatives could be developed further as mitochondrial-related anticancer agents.

Supplementary material

Crystallographic data for the structural analysis have been deposited with the Cambridge Crystallographic Data Centre, CCDC No. 1008721 for 1. The data can be obtained free of charge via http://www.ccdc.cam.ac.uk or from the Cambridge Crystallographic Data Centre, 12 Union Road, Cambridge CB21EZ, UK; fax: (+44) 1223-336-033; or e-mail: deposit@ccdc.cam.ac.uk.

Acknowledgments We thank the financial support from National Science Foundation of China (21271090).

References

1. Osanto S, Poppel HV, Burggraaf J (2013) Future Oncol 9:1271–1281
2. Lavrado J, Borralho PM, Ohnmacht SA, Castro RE, Rodrigues CMP, Moreira R, Dos Santos DJVA, Neidle S, Paulo A (2013) Chem Med Chem 8:1648–1661
3. Qi BH, Mi B, Zhai X, Xu ZY, Zhang XL, Tian ZR, Gong P (2013) Bioorg Med Chem 21:5246–5260
4. Xie YY, Huang HL, Yao JH, Lin GJ, Jiang GB, Liu YJ (2013) Eur J Med Chem 63:603–610
5. Jiang GB, Yao JH, Wang J, Li W, Han BJ, Xie YY, Lin GJ, Huang HL, Liu YJ (2014) New J Chem 38:2554–2563
6. Kruppa M, Konig B (2006) Chem Rev 106:3520–3580
7. Chen QY, Zhou DF, Huang J, Guo WJ, Gao J (2010) J Inorg Biochem 104:1141–1147
8. Frezza C, Gottlieb E (2009) Semin Cancer Biol 19:4–15
9. Monteith GR, Andrew DM, Faddy HM, Robert-Thomson SJ (2007) Nature Rev Cancer 7:519–529
10. Wurtele C, Sanser Q, Lutz V, Waitz T, Tuczek F, Schindler S (2009) J Am Chem Soc 131:7544–7545
11. Li JF, Chen QY (2009) Spectrochim Acta, Part A 73:25–28
12. Romero I, Dubois L, Collomb MN, Deronzier A, Latour JM, Pecaut J (2002) Inorg Chem 41:1795–1806
13. Groni S, Dorlet P, Blain G, Bourcler S, Guillot R, Anxolabehere-Mallart E (2008) Inorg Chem 47:3166–3172
14. López-Lázaro M (2007) Cancer Lett 252:1–8
15. Sheldrick GM (1997) SHELXTL-97, Program for Crystal Structure Solution and Refinement. University of Göttingen, Germany
16. Liu HL, Xu JJ, Dai XM, Shi JB, Xu S, Gao J, Yao QZ, Liu F (2009) J Appl Toxicol 29:489–495
17. Shin BK, Kim MY, Han JH (2010) Polyhedron 29:2560–2568
18. Shin BK, Kim MY, Han JH (2007) Polyhedron 26:4557–4566
19. Chen QY, Huang J, Li JF, Gao J (2008) Chin Inorg Chem 11:1789–1793
20. Waldo GS, Penner-Hahn JE (1995) Biochem 34:1507–1512
21. Boer JW, Feringa BL, Hage RCR (2007) Chim 10:341–354
22. Barynin VV, Hempstead PD, Vagin AA, Artymiak PJ (1997) J Inorg Biochem. 67:196–198
23. Zhou DF, Chen QY, Qi Y, Fu HJ, Li Z, Zhao KD, Gao J (2011) J Inorg Chem 50:6929–6937
24. Weiss JN (1997) FASEB J. 11:835–841
25. Shank M, Barynin VV, Dismukes GC (1994) J Biochem 33:15433–15436
26. Allgood GS, Perry JJ (1986) J Bacteriol 168:563–567
27. Triller MU, Hsieh WY, Pecoraro VL (2002) J Inorg Chem 41:5544–5554
28. Larson EJ, Pecoraro VL (1991) J Am Chem Soc 113:7809–7810
29. Mohammadi-Bardbori A, Ghazi-Khansari M (2007) Toxico Mechan Methods 17:87–91
30. Niesel J, Pinto A, N'Dongo HWP, Merz K, Ott I, Gust R, Schatzschneider U (2008) Chem Commun 15:1798–1800